Acta Crystallographica Section F
Structural Biology and Crystallization Communications
ISSN 1744-3091

Purification, crystallization and halide phasing of a *Streptococcus agalactiae* backbone pilin GBS80 fragment

Krishnan Vengadesan,[a] Xin Ma,[b] Prabhat Dwivedi,[b] Hung Ton-That[b] and Sthanam V. L. Narayana[a]*

[a]Center for Biophysical Sciences and Engineering, School of Optometry, University of Alabama at Birmingham, Birmingham, AL 35294, USA, and [b]University of Texas Health Science Center, Houston, TX 77030, USA

Correspondence e-mail: narayana@uab.edu

Received 18 August 2010
Accepted 22 October 2010

The Gram-positive pathogen *Streptococcus agalactiae* or group B streptococcus (GBS) is the leading cause of bacterial septicemia, pneumonia and meningitis among neonates around the world. The pathogen assembles two types of pili on its surface, named PI-1 and PI-2, that mediate bacterial adherence to host cells. The GBS PI-1 pilus is formed by the major pilin GBS80, which forms the pilus shaft, and two minor pilins GBS104 and GBS52, which are incorporated into the pilus structure. While considerable structural information exists on Gram-negative pili, the structural study of Gram-positive pili is an emerging area of research. Here, the purification, crystallization and initial phasing of the 35 kDa major fragment of the backbone pilin GBS80 are reported. Crystals were obtained in two different space groups: $P2_1$ and $C2$. SAD data collected from an iodide-derivative crystal at the home source were used to obtain initial phases and interpretable electron-density maps.

1. Introduction

Many Gram-positive bacterial pathogens use their cell-wall-anchored pili to initiate adherence to the host cells, which is the key initial step in bacterial colonization. A typical pilus is made up of two or three distinct individual pilins, multiple copies of which assemble to form hair-like appendages on the bacterial cell walls (Mandlik *et al.*, 2008). Gram-negative pilus assembly is well understood (Proft & Baker, 2009); however, the same is not true for Gram-positive bacteria, for which the mechanism of pilus assembly is a relatively recent discovery (Ton-That & Schneewind, 2004; Lauer *et al.*, 2005; Rosini *et al.*, 2006; Dramsi *et al.*, 2006). It has been suggested, mainly from the well studied *Corynebacterium diphtheriae* pilus model (Ton-That & Schneewind, 2004), that the pili are assembled through covalent linkage of individual protein subunits (pilins); this is in contrast to Gram-negative pili, in which they are held together by noncovalent interactions (for a recent review, see Kline *et al.*, 2010). A cysteine transpeptidase called sortase, which is conserved across all Gram-positive bacteria, is implicated in such covalent linkages between the pilin subunits.

Streptococcus agalactiae or group B streptococcus (GBS) causes pneumonia, septicemia and meningitis in neonates and is responsible for significant morbidity and mortality in the United States and Europe (Baker & Edwards, 2001). Genomic analysis of GBS strains (2603V/R, NEM316 and A909) shows the presence of two similar pilus islands (PIs; Rosini *et al.*, 2006; Dramsi *et al.*, 2006). The GBS PI-1 pilus (strain 2603V/R) is built from three pilins GBS80, GBS52 and GBS104. The major pilin GBS80 forms the pilus shaft, while the two minor pilins GBS104 and GBS52 are incorporated into the pilus structure.

The GBS pili are considered to be important targets for vaccine development, since they are important virulence factors for several diseases and take part in multiple functions, including host-cell adhesion (Soriani & Telford, 2010). In addition to facilitating vaccine design, we initiated structural studies on the individual pilin components of GBS in order to understand pilus assembly in Gram-positive bacteria. We have previously reported the structure of the GBS minor pilin GBS52 (Krishnan *et al.*, 2007), which was the first

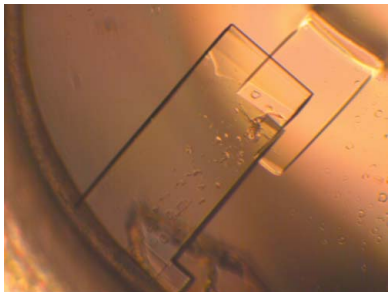

pilin structure to be determined from a Gram-positive bacterium. Recently, several further pilin structures from other Gram-positive organisms have also been reported (Budzik *et al.*, 2009; Kang *et al.*, 2007, 2009; Izoré *et al.*, 2010; Spraggon *et al.*, 2010; Linke *et al.*, 2010). Here, we describe the expression, purification, crystallization and initial phasing procedure that we used for the structure determination of a 35 kDa C-terminal fragment of GBS80, which exhibits poor sequence homology (<18%) to the other backbone pilins Spy0128 from *S. pyogenes* (Kang *et al.*, 2007), SpaA from *C. diphtheriae* (Kang *et al.*, 2009), BcpA from *Bacillus cereus* (Budzik *et al.*, 2009) and RrgB from *S. pneumoniae* (Spraggon *et al.*, 2010).

2. Methods, results and discussion

2.1. Cloning, expression and purification

S. agalactiae 2603V/R was obtained from the American Type Culture Collection (ATCC). The primers 5′-AAAGGATCCAGAGCTGCAGAAGTGTCACA-3′ and 5′-AAAGGATCCTTAACGTTTGTTGTTTTTAATTGTATC-3′ were used to PCR-amplify the sequence of GBS *gbs80* (coding for Arg36–Arg518) from chromosomal DNA of GBS strain 2603V/R (locus tag SAG0645). The DNA fragment was cloned into pQE30 according to a published protocol (Mandlik *et al.*, 2007). After verification by DNA sequencing, the resulting plasmid pHTT110 was transformed into *Escherichia coli* XL1-Blue.

GBS $GBS80_{36–518}$ with an N-terminal His tag (MRGSHHHHHHGS) was expressed and purified as follows. Overnight cultures (20 ml) of stationary-phase *E. coli* were used to inoculate 1 l Luria–Bertani (LB) broth supplemented with 100 µg ml^{-1} ampicillin. The cells were allowed to grow at 310 K until the culture reached an $OD_{600\,nm}$ of ∼0.6. Protein expression was induced by the addition of isopropyl β-D-1-thiogalactopyranoside (IPTG) to a final concentration of 0.2 m*M* and the culture was incubated overnight at 303 K. The cells were harvested by centrifugation and resuspended in lysis buffer [50 m*M* phosphate pH 7.4, 300 m*M* NaCl, 5%(*v*/*v*) glycerol, 5 m*M* imidazole] containing EDTA-free protease-inhibitor cocktail tablets (Roche). The cells were lysed by passage three times through a French press (76 MPa). Insoluble debris was removed by centrifugation at 48 384*g* for 20 min at 277 K and the supernatant was applied onto a 10 ml $NiCl_2$-charged HiTrap chelating column (two 5 ml columns were connected serially). The columns were connected to an FPLC system (Pharmacia) and washed with ten bed volumes of buffer *A* [50 m*M* phosphate pH 7.4, 300 m*M* NaCl, 5% (*v*/*v*) glycerol, 5 m*M* imidazole]. The bound protein was eluted with a linear gradient of 0–300 m*M* imidazole to elution buffer *B* (300 m*M* imidazole in buffer *A*). Fractions containing the desired protein, as determined by SDS–PAGE, were pooled and dialyzed against 20 m*M* Tris–HCl pH 7.4, 150 m*M* NaCl, 2 m*M* EDTA. The dialyzed protein was concentrated using an Amicon ultrafiltration system and applied

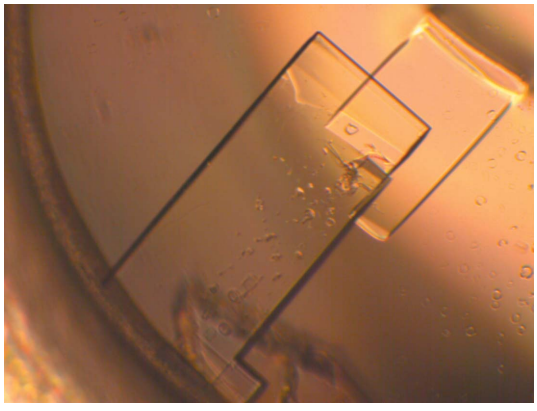

Figure 1
Example of native crystals (0.5 × 0.3 × 0.1 mm in size) of the 35 kDa fragment of GBS80 (chymotrypsin-digested) obtained in 25%(*w*/*v*) PEG MME 2000, 0.1 *M* MES pH 5.5 after 21 d at 295 K.

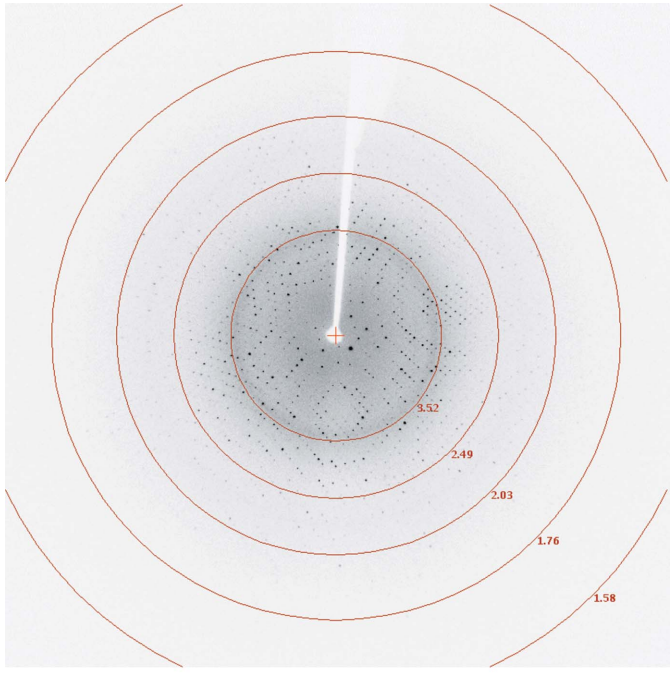

(*a*)

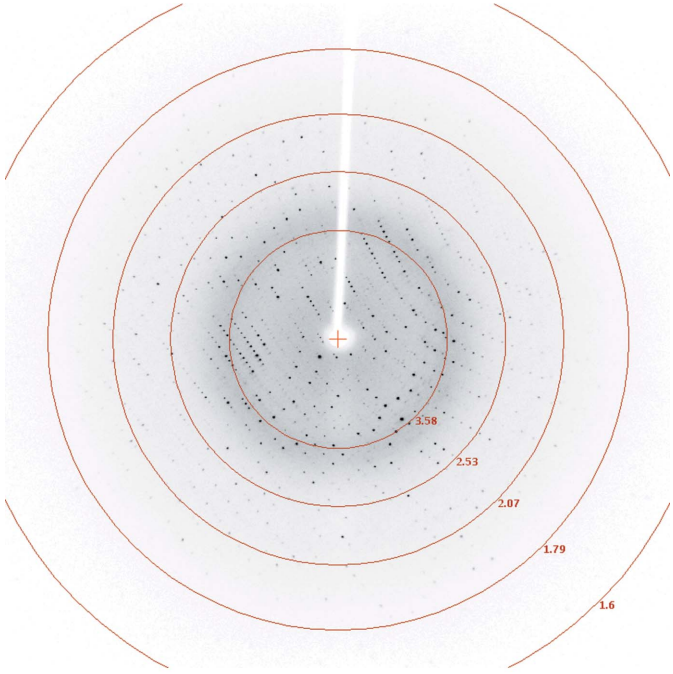

(*b*)

Figure 2
(*a*) X-ray diffraction image from crystals of the chymotrypsin-digested native 35 kDa fragment of GBS80 collected on an R-AXIS IV imaging-plate detector mounted on an in-house Rigaku rotating-anode X-ray generator operated at 100 mA and 50 kV. (*b*) X-ray diffraction image from crystals of the $CaCl_2$-treated 35 kDa fragment of GBS80.

Table 1
Data-collection and processing statistics.

Values in parentheses are for the highest resolution shell.

	Native (chymotrypsin-treated)	Native ($CaCl_2$-treated)	Derivative (NaI-soaked)
No. of crystals	1	1	1
Beamline	In-house	In-house	In-house
Wavelength (Å)	1.5418	1.5418	1.5418
Detector	R-AXIS IV image plate	R-AXIS IV image plate	R-AXIS IV image plate
Crystal-to-detector distance (mm)	100	105	150
Rotation range per image (°)	1	0.75	1
Total rotation range (°)	190	296	360
Exposure time per image (s)	300	300	300
Resolution range (Å)	40–1.7 (1.76–1.70)	40–1.7 (1.76–1.70)	40–2.0 (2.07–2.00)
Space group	$P2_1$	$C2$	$P2_1$
Unit-cell parameters (Å, °)	a = 69.9, b = 60.3, c = 80.4, β = 101.6	a = 130.5, b = 34.7, c = 74.6, β = 93.3	a = 34.9, b = 59.7, c = 80.8, β = 101.6
Mosaicity (°)	0.4	0.4	0.5
Total No. of measured intensities	200661	158279	138772
Unique reflections	71940	37173	21409
Multiplicity	2.8 (2.7)	4.3 (4.1)	6.5 (5.9)
Mean $I/\sigma(I)$	8.3 (2.5)	26.7 (6.5)	18.9 (9.0)
Completeness (%)	99.7 (100)	99.8 (100)	96.7 (87.1)
χ^2	0.97 (1.16)	0.97 (1.10)	0.95 (1.03)
R_{merge} (%)†	6.8 (37.2)	2.8 (17.1)	5.6 (15.2)
Overall B factor from Wilson plot (Å^2)	19.3	19.8	23.2
No. of molecules in the asymmetric unit	2	1	1
R_{anom} (%)‡	—	—	3.2 (5.3)
Phasing (for all data)			
Phasing power§	—	—	1.3
R_{Cullis}§	—	—	0.75
Figure of merit	—	—	0.33

† $R_{merge} = \sum_{hkl}\sum_i |I_i(hkl) - \langle I(hkl)\rangle| / \sum_{hkl}\sum_i I_i(hkl)$, where the $I_i(hkl)$ are the intensities of symmetry-related reflections and $\langle I(hkl)\rangle$ is the average intensity over all observations. ‡ $R_{anom} = \sum |I^+(h) - I^-(h)| / \sum [I^+(h) + I^-(h)]$, where $I^+(h)$ and $I^-(h)$ are the Bijvoet pairs of $I(h)$. § From *autoSHARP* for acentric reflections.

onto an S-200 (26/60) Sephacryl gel-filtration column in a buffer consisting of 20 m*M* Tris–HCl pH 7.4, 150 m*M* NaCl, 40 m*M* L-Arg, 40 m*M* L-Glu, 2 m*M* EDTA. After desalting in 20 m*M* Tris–HCl pH 7.4, the protein was further purified on a HiTrap Q column with elution buffer consisting of 20 m*M* Tris–HCl pH 7.4, 1 *M* NaCl. The purified GBS80 was concentrated to 15–60 mg ml^{-1}, but crystallization trials were unsuccessful. Partial degradation of the purified protein was noticed after storage. The inclusion of protease inhibitors did not stop the degradation completely. Therefore, limited proteolysis by trypsin was attempted in order to obtain a stable fragment, but yielded several nonspecific smaller fragments. However, proteolysis by α-chymotrypsin after optimization (overnight digestion at a 1:100 ratio at room temperature in digestion buffer consisting of 30 m*M* Tris–HCl pH 7.4, 100 m*M* NaCl) yielded a stable 35 kDa fragment. The inhibitor PMSF was added to the digested GBS80 to a concentration of 0.5 m*M* and it was then subjected to size-exclusion chromatography using an S-200 (16/60) column in crystallization buffer (20 m*M* Tris–HCl pH 7.0, 100 m*M* NaCl). N-terminal sequencing suggested that the cleavage occurred at the pilin motif (YPKN) between Lys199 and Asn200. Molecular-weight calculation from the sequence (Asn200–Arg518) and SDS–PAGE confirmed that there was no C-terminal cleavage. Moreover, the initial electron-density map calculated from the iodide SAD phasing as described below clearly shows the presence of the C^α trace for the C-terminal residues of GBS80.

2.2. Crystallization

The purified GBS80 35 kDa fragment was concentrated to 10 mg ml^{-1} in 20 m*M* Tris–HCl pH 7.0, 100 m*M* NaCl and subjected to crystallization by the sitting-drop vapor-diffusion method with the help of a Crystal Phoenix robot (Art Robbins Instruments) as well as manually by the hanging-drop crystallization method using various commercial crystal screens. Plate-like diffraction-quality crystals appeared after three weeks in four conditions. Large crystals suitable for X-ray diffraction analysis were obtained in an optimized condition consisting of 2 µl protein solution in 20 m*M* Tris–HCl pH 7.0, 100 m*M* NaCl mixed with 2 µl reservoir solution and equilibrated against a 1.0 ml reservoir of 0.1 *M* MES pH 5.5, 25%(*w*/*v*) PEG MME 2000 at 295 K (Fig. 1). Another batch of GBS80 purified using a similar protocol and treated with 10 m*M* $CaCl_2$ as an additive also degraded to a 35 kDa fragment. Crystals of the $CaCl_2$-treated GBS80 fragment were obtained using the same conditions [0.1 *M* MES pH 5.5, 25%(*w*/*v*) PEG MME 2000] but belonged to a different space group (see below).

2.3. Data collection

Native diffraction data were collected to 1.8 Å resolution (Fig. 2*a*) on an R-AXIS IV imaging-plate detector mounted on an in-house Rigaku rotating-anode X-ray generator operating at 100 mA and 50 kV. Diffraction data were collected using one crystal over a range of 190° with 1° steps, using 20%(*v*/*v*) ethylene glycol (EG) as a cryoprotectant. The data were processed with *d*TREK* (Pflugrath, 1999) and crystallographic data statistics are presented in Table 1. Diffraction data from $CaCl_2$-treated GBS80 crystals were also collected in-house (Table 1) using 20%(*v*/*v*) EG as a cryoprotectant (Fig. 2*b*).

The native GBS80 crystals belonged to the monoclinic space group $P2_1$, with unit-cell parameters a = 69.9, b = 60.3, c = 80.4 Å, β = 101.6°. The V_M calculation (calculated V_M of 2.4 Å^3 Da^{-1} and solvent content of 48%) suggested the presence of two molecules in the asymmetric unit. Analysis of the diffraction data using *SFCHECK* (Collaborative Computational Project, Number 4, 1994) suggested the presence of pseudo-translational symmetry (x + 1/2, y, z). The $CaCl_2$-treated GBS80 fragment crystals belonged to the monoclinic space group $C2$, with unit-cell parameters a = 130.3, b = 34.6, c = 74.6 Å, β = 93.3°. The V_M calculation (V_M of 2.4 Å^3 Da^{-1} and solvent content of 49%) suggested the presence of one molecule in the asymmetric unit.

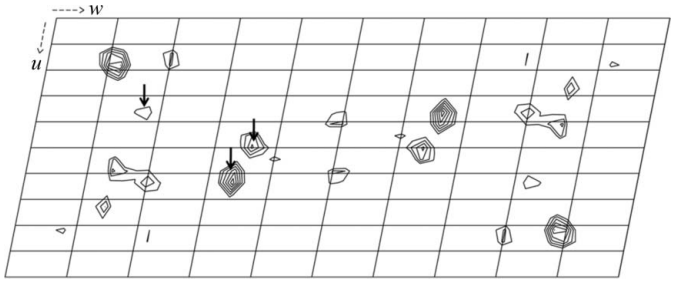

Figure 3
The $(u, 1/2, w)$ Harker section of the anomalous difference Patterson map $(F^+ - F^-)$ calculated and plotted using the *FFT* and *NPO* programs from *CCP*4 linked to *autoSHARP* with data between 20 and 5 Å resolution. The contour levels are at 0.4 r.m.s. intervals, starting at 1.5 r.m.s. above the mean density. The arrows show the three iodide sites with high occupancies identified in the initial search using *autoSHARP*.

2.4. Heavy-atom derivatives and initial phasing

The halide quick-soaking method proposed by Dauter *et al.* (2000) was used for phasing, since molecular replacement and a search for traditional heavy-atom derivatives were not successful. The crystallized fragment of GBS80 contains only one Met residue, therefore we did not attempt to produce its recombinant SeMet derivative. The theoretical pI of the crystallized fragment is 5.3 and the 35 kDa fragment of GBS80 contains four Arg and 41 Lys (14%) residues. Anticipating the potential for binding halide anions, we initiated attempts to introduce them by screening various halide anions and alkali-metal cations such as KI, NaI and CsCl; the iodide derivative obtained using NaI showed significant anomalous signal.

The iodine derivatives were prepared either by directly soaking crystals of the 35 kDa fragment of GBS80 in reservoir solution with NaI added or in cryoprotectant solution containing 200 m*M* NaI for a short time of between 1 and 2 min. During the soaking, no visible cracking of the crystals was observed. Diffraction data for the iodide derivatives were collected at a wavelength of 1.5418 Å at the home source data-collection facility (Table 1) and the data were processed with *d*TREK* (Pflugrath, 1999). The unit-cell volume of the iodide-derivative crystals was half of that of the native crystal in space group $P2_1$ (Table 1), with one molecule in the asymmetric unit, and the crystal had no pseudo-translational symmetry. However, the change in unit-cell parameters was not a consequence of the iodide soaking, as a few native crystals were also found that diffracted to <2 Å resolution with smaller unit-cell parameters. The anomalous signal of the iodide derivative was evaluated using the *autoSHARP* software (Vonrhein *et al.*, 2007); three iodide sites were identified in the initial anomalous difference Patterson maps (Fig. 3) and seven additional sites were identified in the second round of residual map interpretation. Model building with the help of *Coot* and *REFMAC* from the *CCP*4 suite (Collaborative Computational Project, Number 4, 1994) is in progress and will be presented elsewhere.

3. Conclusions

The GBS80 fragment was purified and crystallized in two conditions. Molecular replacement and a conventional heavy-atom derivative search for initial phasing were not successful. The high content of Lys and Arg residues in the GBS80 fragment prompted us to try halide soaking (Dauter *et al.*, 2000). It has been reported that halide anions bind tightly (Dauter *et al.*, 2000) as indicated by their high anomalous difference peaks, good occupancies and low *B* factors. Of the halides tried, NaI soaking yielded good phasing information, while soaking in KI and CsCl resulted in crystal cracking. The use of a home source X-ray facility and simple halide quick-soaking combined with automatic structure-determination software is a powerful method that is worth trying as an alternative to a conventional MIR search for heavy-atom derivatives.

This work was supported by NIH grants to HT-T (AI061381) and SVLN (AI073521).

References

Baker, C. J. & Edwards, M. S. (2001). *Infectious Diseases of the Fetus and Newborn Infant*, edited by J. S. Remington & J. O. Klein, pp. 1091–1156. Philadelphia: W. B. Saunders.
Budzik, J. M., Poor, C. B., Faull, K. F., Whitelegge, J. P., He, C. & Schneewind, O. (2009). *Proc. Natl Acad. Sci. USA*, **106**, 19992–19997.
Collaborative Computational Project, Number 4 (1994). *Acta Cryst.* D**50**, 760–763.
Dauter, Z., Dauter, M. & Rajashankar, K. R. (2000). *Acta Cryst.* D**56**, 232–237.
Dramsi, S., Caliot, E., Bonne, I., Guadagnini, S., Prevost, M. C., Kojadinovic, M., Lalioui, L., Poyart, C. & Trieu-Cuot, P. (2006). *Mol. Microbiol.* **60**, 1401–1413.
Izoré, T., Contreras-Martel, C., El Mortaji, L., Manzano, C., Terrasse, R., Vernet, T., Di Guilmi, A. M. & Dessen, A. (2010). *Structure*, **18**, 106–115.
Kang, H. J., Coulibaly, F., Clow, F., Proft, T. & Baker, E. N. (2007). *Science*, **318**, 1625–1628.
Kang, H. J., Paterson, N. G., Gaspar, A. H., Ton-That, H. & Baker, E. N. (2009). *Proc. Natl Acad. Sci. USA*, **106**, 16967–16971.
Kline, K. A., Dodson, K. W., Caparon, M. G. & Hultgren, S. J. (2010). *Trends Microbiol.* **18**, 224–232.
Krishnan, V., Gaspar, A. H., Ye, N., Mandlik, A., Ton-That, H. & Narayana, S. V. (2007). *Structure*, **15**, 893–903.
Lauer, P., Rinaudo, C. D., Soriani, M., Margarit, D., Maione, D., Rosini, R., Taddei, A., Mora, M., Rappuoli, R., Grandi, G. & Telford, J. L. (2005). *Science*, **309**, 105.
Linke, C., Young, P. G., Kang, H. J., Bunker, R. D., Middleditch, M. J., Caradoc-Davies, T. T., Proft, T. & Baker, E. N. (2010). *J. Biol. Chem.* **285**, 20381–20389.
Mandlik, A., Swierczynski, A., Das, A. & Ton-That, H. (2007). *Mol. Microbiol.* **64**, 111–124.
Mandlik, A., Swierczynski, A., Das, A. & Ton-That, H. (2008). *Trends Microbiol.* **16**, 33–40.
Pflugrath, J. W. (1999). *Acta Cryst.* D**55**, 1718–1725.
Proft, T. & Baker, E. N. (2009). *Cell. Mol. Life Sci.* **66**, 613–635.
Rosini, R., Rinaudo, C. D., Soriani, M., Lauer, P., Mora, M., Maione, D., Taddei, A., Santi, I., Ghezzo, C., Brettoni, C., Buccato, S., Margarit, I., Grandi, G. & Telford, J. L. (2006). *Mol. Microbiol.* **61**, 126–141.
Soriani, M. & Telford, J. L. (2010). *Future Microbiol.* **5**, 735–747.
Spraggon, G., Koesema, E., Scarselli, M., Malito, E., Biagini, M., Norais, N., Emolo, C., Barocchi, M. A., Giusti, F., Hilleringmann, M., Rappuoli, R., Lesley, S., Covacci, A., Masignani, V. & Ferlenghi, V. (2010). *PLoS ONE*, **5**, e10919.
Ton-That, H. & Schneewind, O. (2004). *Trends Microbiol.* **12**, 228–234.
Vonrhein, C., Blanc, E., Roversi, P. & Bricogne, G. (2007). *Methods Mol. Biol.* **364**, 215–230.